



Wind damage on citrus fruit study: Wind tunnel tests

José Cataldo^a, Valeria Durañona^a, Rodolfo Pienika^{a,*}, Pablo Pais^a, Alfredo Gravina^b

^a Instituto de Mecánica de los Fluidos e Ingeniería Ambiental, Facultad de Ingeniería, Universidad de la República, Montevideo, Uruguay

^b Departamento de Producción Vegetal, Facultad de Agronomía, Universidad de la República, Montevideo, Uruguay

ARTICLE INFO

Article history:

Received 16 March 2012

Received in revised form

28 December 2012

Accepted 16 January 2013

Keywords:

Wind damage

Citrus fruit

Turbulence

Small-scale

Wind tunnel

ABSTRACT

The interaction between citrus trees and wind was studied in a wind tunnel. Wind flows at mean velocities between 1 m/s and 3 m/s were simulated, as well as with different energy content at turbulence small-scale. The wind modeling methodologies applied to do so are presented. At a mean velocity, if the turbulence small-scales' energy is high, the consequent leaves' displacement is greater than when the former is low, decreasing the contact time between the leaf and the fruit. Nevertheless, the rest of the tree components do not present significant differences in their responses. This led us to infer that the greater energy at turbulence small-scales could be correlated with a lower period of time a leaf rubs against an adjacent fruit. Therefore, leaves' mechanical action and the consequent damage could be reduced increasing the turbulence small-scale energy content.

© 2013 Elsevier Ltd. All rights reserved.

1. Introduction

In Uruguay, between 10% and 40% of damage on citrus fruits is caused by the deteriorative actions of wind, which results in the discarding of the fruit from exportation, as reported by Gravina (1998), Martínez (1995) and Montes (personal communication). The main cause of such damage, which affects the appearance of fruits and produces huge economic losses is the hitting, rubbing and cutting produced by branches and leaves moved by the wind, causing scars and brazes on the fruit peel.

In 2004, the Crop Production Department of the School of Agronomy together with the Institute of Fluids' Mechanics and Environmental Engineering of the School of Engineering, both from Universidad de la República—Uruguay, undertook a research program aimed to analyze wind damage on citrus fruits in Uruguay, whose main objective was to provide a description of wind damage on citrus fruits from a physical and biological point of view. As a result, a design criterion for a wind protection system was proposed, and a theoretical model to describe the movement of the trunk, branches and leaves was developed. In particular, to describe the fruit peel damage process, it was necessary to understand the interaction between wind and trees.

Quoting Green (1968), damage on citrus fruit caused by the wind is associated to high mean wind velocity (greater than 5 m/s). In order to solve this issue, farmers implement several measures, such as using live wind fences (Owen-Turner and

Hardy, 2006), which consist of tree rows located around the orchards. The live fences would decrease the mean wind velocity. Notwithstanding, this strategy does not actually imply a reduction in the damage caused to the fruit. Alternatively, other farmers use artificial wind fences consisting of plastic screens (Freeman, 1976; Green, 1968; Owen-Turner and Hardy, 2006) with small mesh size (2 mm–3 mm). But this strategy does not render positive results.

From the observation of the movements of a tree, different displacement scales could be identified, such as leaves, branches or trunk displacement.

These different scales of movement could be associated to the damage occurred through the different fruit growing stages. When fruits are in the early growing stages (smaller than 1 cm), their surface presents irregularities on which adjacent leaves specially the old ones tend to rub them (small scale movement), whereas, the damage in adult fruits would be associated to the movement of branches, which hit the fruits (large scale movement). Following the evolution of the fruit damage process conducted by the agronomy group in charge of this project, the damage produced during the early growing stages was identified as the most significant since it is the one that produces rejection from exportation as it is also quoted in Brodrick (1970), Campbell (1967), Dodson (1966), Freeman (1976), and Gravina et al. (2005). Therefore, the most significant damage is that associated to the movement of leaves. We consider as an important target to understand how the different parts of a tree, specially the leaves, are moved by the wind.

Several authors that describe the large-scale turbulence produced by the interaction of trees and wind such as Brunet et al.

* Corresponding author. Tel.: +598 2 7115278; fax: +598 2 7115277.
E-mail address: rpienika@fing.edu.uy (R. Pienika).

(2003), Finnigan and Brunet (1995), Gardiner (1995), Ruck and Adams (1991), Scarabino (2005) and Shaw (2006) can be quoted. However the large-scale turbulence could be associated, principally, to large scale tree's movements. The interaction between citrus trees and wind, especially the effect of the small-scale turbulence at low mean wind velocity, is scarcely reported. These turbulence scales would be associated to small-scale movements of a tree.

Within the framework of this research program, we intended to provide a description of the orchard's flow field, the mean and the turbulent velocity component included. From field measurements we characterized the flow in the orchard. Then the response of different tree-components was analyzed in wind tunnel tests.

A citrus tree was tested in the wind tunnel of the Institute of Fluids' Mechanics and Environmental Engineering of the School of Engineering, from Universidad de la República—Uruguay. The main objective of the tests was to study the response of different tree components, under turbulent flows' action and link it with the wind flow characteristics existing inside a citrus orchard.

In order to simulate wind flow orchard's characteristics, several turbulence production systems were studied.

The displacements (i.e. responses) of trunk, branches and leaves under wind action, and the wind velocity were simultaneously measured. Moreover, the aforementioned displacements were visualized and recorded with a digital video camera.

A theoretical model linking the deflection of the tree components and the velocity of the oncoming wind flow was studied.

2. Material and methods

2.1. Specimen tree description

A young specimen of 'Navelate' oranges was obtained with a height and foliage width to facilitate its location in the wind tunnel's test section. The wind tunnel is an atmospheric boundary layer and open suction type one, whose test section presents a cross section of 2.25 m width, 2.10 m high and 17 m long.

The tree was 106 cm high, whilst the leaves' size varied from 50 mm length and 28 mm width to 157 mm length and 89 mm width (see Fig. 1).

The orchard's trees height (prototype) and the model tree height ratio were roughly 3, whilst the leaves' dimensions did not present significant differences between such trees. Therefore, the tree located in the wind tunnel constituted a scaled distorted model of a typical tree found in a citrus orchard.



Fig. 1. Specimen tree view, inside the wind tunnel.

2.2. Turbulent flow simulation

The adequate simulation of atmospheric flow's vortex structures interacting principally with leaves was prioritized. Nevertheless, all turbulence scales being modeled were verified.

The vortices with scales equal to or lower than a leaf's size and the ones with scales equal to or greater than the branches, in the studied process in this paper, will be defined as the turbulence small-scale and big-scale, respectively.

The turbulence small-scale energy content was characterized with the turbulence small-scale parameter defined by Melbourne (1979). Such parameter is defined as

$$\xi = \frac{f_{ss} S_u(f_{ss})}{\sigma_u^2} I_u^2 \times 10^6 = \frac{\text{Energy}(\lambda_{ss})}{\text{Energy}(\text{means flow})} \quad (1)$$

where $I_u = \sigma_u / \bar{U}$ is the turbulence intensity, σ_u and \bar{U} are the standard deviation and mean of wind velocity respectively, f_{ss} is the characteristic frequency of small-scale turbulence (defined by applying Taylor's hypothesis as $f_{ss} = \bar{U} / \lambda_{ss}$), λ_{ss} is the incident flow vortices' length-scale exchanging the greatest part of energy with leaves-size scale vortices, and S_u is the longitudinal velocity power spectral density.

From previous turbulence spectral analysis of orchards' wind velocity measurements (Cataldo et al., 2011), two ranges of values of such parameter were identified.

The first range of turbulence small-scale parameter values is between 800 and 2000 and the second one is between 3000 and 5000. In the orchard, longitudinal integral length scale of the order of trees' height (~ 3 m) was found. Then, simulations of wind flows with turbulence small-scale parameter lying in each of the aforementioned ranges were performed.

In order to perform the wind tunnel flow simulation, several turbulence production systems were studied. Fences with different mesh sizes and porosities, at different distances upstream of the tree, were installed following Batchelor (1960), Farell and Youssef (1992), Groth and Johansson (1988), Richardson (1989) and Richardson and Richards (1995). Also, spires with two different heights were used. Two mean velocity values, one close to 1 m/s and the other one close to 3 m/s, were selected. As it is shown in Cataldo et al., 2011 these velocity values are typical in a citrus orchard.

A hot wire anemometer TSI, model IFA100 with three channels, was used to measure wind velocity. The anemometer was calibrated in the wind tunnel of the School of Engineering, which has all its instruments traceable with the International System. A bent probe was used. The probe positioning was achieved with the use of a lancet moved by a four-degrees-of-freedom positioning robot. Velocity signals were processed with a specific developed program, obtaining mean value, standard deviation and power spectral density of the fluctuating velocity component calculated following Newland (1984). Most significant turbulence parameters, such as longitudinal integral length scales and the energy content at turbulence small-scales, were obtained from the spectra.

From the analyzed alternatives two turbulence production systems were selected.

A 380 mm mesh-size fence, with rectangular cross section of 120 mm width bars, located 165 cm upstream of the tree position, was a first simulation system. With such system a flow with high energy content at small-scales was well simulated. ξ values between 4236 and 6513 and an average turbulence intensity value of 30% were obtained.

A 125 mm mesh-size fence, with circular cross section of 25 mm diameter bars, located 165 cm upstream of the grid, and six evenly spaced triangular spires, was used as a second simulation system. With such system, a flow with low energy content at

small-scales was well simulated. § values between 671 and 2216 and an average turbulence intensity value of 18% were obtained.

With both systems, we obtained flows with the highest energy content vortices with scales of interest (leaf's size), i.e. the turbulence small-scale.

2.3. Strain measurements

Strain gages were attached to different parts of the tree, to measure their strain under wind loading. Each strain gage in a balanced quarter bridge connection scheme was installed. The unbalanced voltage when a tree component is deformed was acquired.

A National Instruments data logger system based on a chassis NI SCXI-1000, with a signals conditioner NI SCXI-1600, a transducer NI SCXI-1122, and a 16 channel terminal block NI SCXI-1322 was used. In the present test five previously calibrated channels were used.

The calibration consisted in loading a particular branch, calculating the strain at a specific position of the branch from deflections measurements with a micrometer (following Popov, 1998) and comparing this result with the strain measured with a strain gage attached at the same specific position of the branch. A calibration factor C was obtained for each channel of the data logger, as the relation between both strain values.

Four strain gages were attached to the tree: one on the trunk, two on boughs and the last one on a petiole. All strain gages were positioned around the middle of each tree component.

The analyzed tree components presented the dimensions that are in Table 1.

Also, a reference strain gage was attached to a piece of wood, free of deformation, but under the same temperature gradient of the other four strain gages, for the purpose of temperature compensation (Moore et al., 2005).

The tree was submitted to different turbulent flows. Strain and velocity data were simultaneously measured. The strain data sampling rate was settled at 400 Hz and the sampling time was 163.84 s, whilst the velocity data sampling rate was settled at 1000 Hz and the sampling time was 65.536 s. In both cases, a total of 65,536 data were obtained.

Previous to wind tunnel tests, a damping test was done, in order to obtain the resonance frequency and damping ratios of each tree component.

2.4. Calculation of deflection

Following Hook's law the relation between strain and deflection of a beam is linear. Also, as suggested by Moore et al. (2005), "Within the range of linear-elastic material behavior, the strain in a tree stem or branch should also be linearly proportional to displacement."

First of all, measured voltage values were corrected by temperature compensation. Then the true strain values were calculated multiplying the measured strain (obtained from the temperature-compensated voltage values) by the calibration factor C.

Table 1
Dimensions of several tree components.

Tree component	Mean diameter (mm)	Length (mm)
Trunk	16.8	375
Bough 1	7.65	200
Bough 2	9.15	200
Petiole	3.1	32

Then, least squares regressions were used to fit a linear model for each component (Moore et al., 2005; James and Kane, 2008). These linear models were used in the wind tunnel tests, to obtain the deflections from the strains measurements.

Finally, the fluctuant components of deflections were calculated as a first order strain fluctuation function.

2.5. Relation between deflection spectrum and velocity spectrum

Frequency response of different components of the tree was investigated through spectral analysis. Theoretical relationship linking the spectrum of the fluctuating deflection (S_x) and the spectrum of the turbulent velocity (S_u) is quoted in Holmes (2001), for the case of single-degree-of-freedom systems. Similar models could be fitted to the case of the different components of a tree, as quoted in Moore (2002) and James and Kane (2008). Such relation could be expressed as follows:

$$S_x(f) = \frac{1}{k^2} \frac{4\bar{D}^2}{\bar{U}^2} |H(f)|^2 \chi^2(f) S_u(f) \quad (2)$$

where k is the spring stiffness, \bar{D} is the mean drag force, \bar{U} is the mean wind velocity, $|H(f)|^2$ is the mechanical admittance (Clough and Penzien, 1993; Moore, 2002), and $\chi^2(f)$ is the aerodynamic admittance (Baker, 1995; Moore, 2002).

3. Results and discussions

3.1. Damping tests' results

From damping tests the strain evolution shows a damped sinusoidal shape. The waves' frequency corresponds to the resonance frequency (f_{res}) of each part of the tree. From the same curves, the damping ratio (ξ) of each tree component could be deduced. Table 2 resumes these values.

3.2. Wind tunnel tests' results

Spectral density curves of velocity fluctuations along with spectral density curves of deflection fluctuations, for some parts of the tree, under certain turbulent flows obtained from measurements, are shown in Figs. 2–4. The effect of both admittances can be appreciated, and a peak in S_x curves could be identified as the resonance frequency of the corresponding tree component, following the premise of Section 2.5.

Qualitatively and quantitatively the measurements results follow the theoretical model predicted in Section 2.5.

Values of resonance frequency (f_{res}) estimated from the spectral peak and the deflection's quadratic mean (σ_x^2), for each part of the tree under different flows actions (\bar{U} , σ_u^2 , and §), are shown in Tables 3 and 4 for low and high small-scale energy content, respectively. In each case, three flows with different mean velocities were tested, but special attention we will devote to results obtained for mean velocity equal to 1 m/s. Such velocity is most frequently presented inside citrus orchards at trees' height (Cataldo et al., 2011).

The petiole movement's amplitude ($\sim \sigma_x^2$) in the high small-scale energy test resulted almost a hundred times greater than in the low small-scale energy case. On the other hand, the trunk and

Table 2
Values of resonance frequencies and damping ratios.

	Trunk	Bough 1	Bough 2	Petiole
f_{res} (Hz)	1.7	3.3	3.3	3.7
ξ	0.144	0.093	0.091	0.078

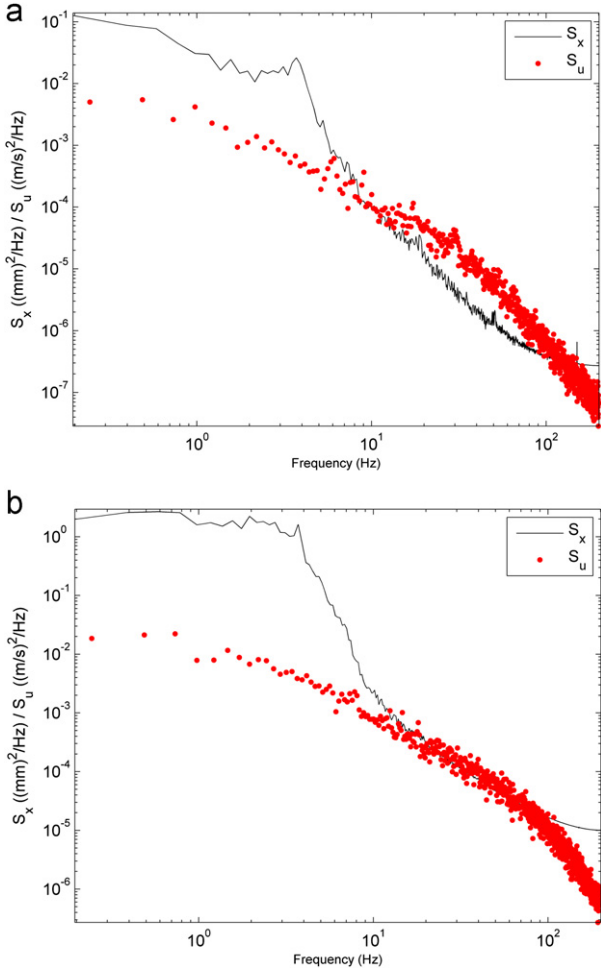


Fig. 2. Spectral density curves of velocity and deflection, for the petiole, with 1 m/s flow and (a) low small-scale energy, and (b) high small-scale energy.

boughs' displacements did not present relevant differences between the low and high small-scale energy tests.

As a consequence, when a low small-scale energy flow blows around a tree, the gap between tree components is very small, although such components may be moving in opposite sense. When a high small-scale energy flow blows around the tree, the petiole displacement's amplitude increases by two orders of magnitude while the displacement of other parts does not increase with significance. As a consequence the leaves are separated from other parts of the tree for a relatively long period of time.

We guessed the order of the contact time between a leaf and an adjacent fruit, under both energy levels. We proposed the following criterion: if the leaf's movement presents amplitude smaller than 10% of the fruit size (~ 1 mm), the leaf and the adjacent fruit would be in contact, while when such amplitude is greater than 1 mm there would be no contact between them. Following the aforementioned criterion the contact time was assessed as 94% of the total time, for the low small-scale energy test, whilst it decreased to 21% for the high small-scale energy test. The same results from wind tunnel visualizations were observed. Then, a greater time contact in a flow with low energy content at small-scale turbulence would be obtained than in a flow with high energy. As a consequence, a greater damage would be awaited in the first kind of flows.

3.3. Dimensional analysis

To identify the most significant variables in the leaves' response a dimensional analysis was performed. The variables

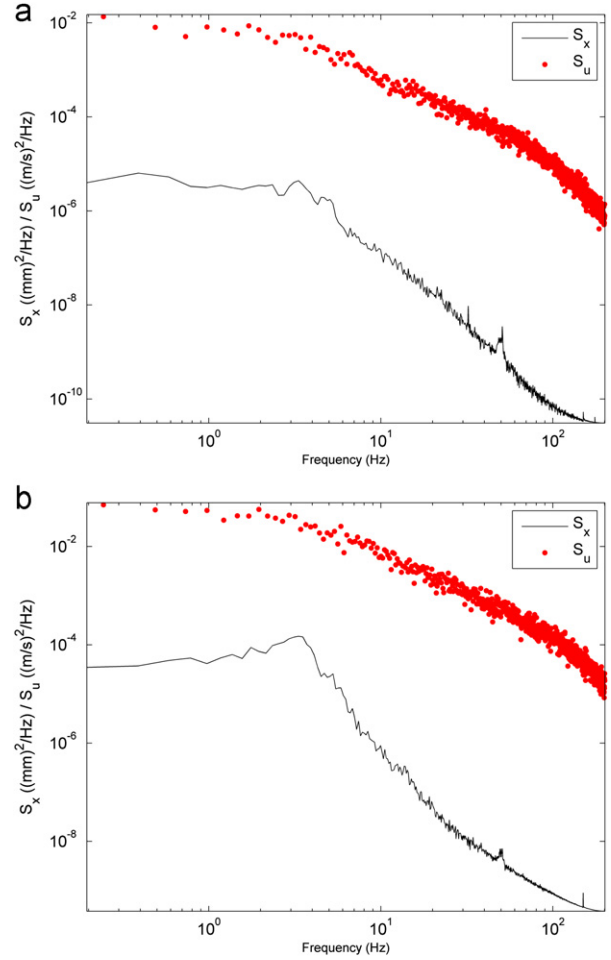


Fig. 3. Spectral density curves of velocity and deflection, for bough 1, with 2 m/s flow and (a) low small-scale energy, and (b) high small-scale energy.

involved in the leaves' movement are the following: deflection's quadratic mean (σ_x^2), the resonance frequency of the tree component (f_{res}) as a scale of the small-scale turbulence frequency, the wind mean velocity (\bar{U}), the air kinematic viscosity (ν_{air}), the longitudinal velocity power spectral density at the resonance frequency $S_u(f_{res})$, and the tree component's mean diameter (ϕ). A relationship between the aforementioned magnitudes is assumed as follows:

$$\sigma_x^2 = F(f_{res}, \bar{U}, \nu_{air}, S_u(f_{res}), \phi) \tag{3}$$

In a first guess we used \bar{U} and ϕ as fundamental magnitudes, but we didn't find a clear-cut relation between the dimensionless parameters. Then, we selected ν_{air} and f_{res} as fundamental magnitudes and the following dimensionless numbers could be deduced: $\sigma_x^2 / (\nu_{air} / f_{res})$, $\bar{U} / \sqrt{\nu_{air} f_{res}}$, $\phi / \sqrt{\nu_{air} / f_{res}}$ and $S_u(f_{res}) / \nu_{air}$. The relation between the dimensionless parameter would be as follows:

$$\frac{\sigma_x^2}{(\nu_{air} / f_{res})} = G\left(\frac{\bar{U}}{\sqrt{\nu_{air} f_{res}}}, \frac{S_u(f_{res})}{\nu_{air}}, \frac{\phi}{\sqrt{\nu_{air} / f_{res}}}\right) \tag{4}$$

Then, we analyzed the dependence of the variable $\sigma_x^2 / (\nu_{air} / f_{res})$ with the independent variables. We found a clear dependence of $\sigma_x^2 / (\nu_{air} / f_{res})$ with the variable $S_u(f_{res}) / \nu_{air}$ as it is shown in Fig. 5. In this figure $\phi / \sqrt{\nu_{air} / f_{res}}$ appears as a parameter.

An upward tendency in the petiole's deflection when the energy content of vortices at petiole's resonance frequency is increased can be observed in Fig. 5. Also, an upward tendency

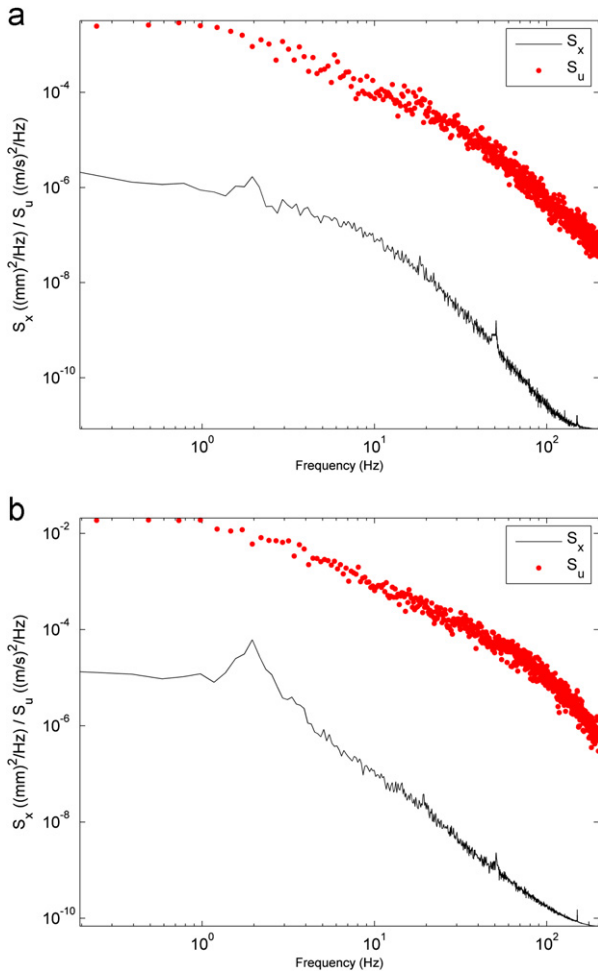


Fig. 4. Spectral density curves of velocity and deflection, for the trunk, with 1 m/s flow and (a) low small-scale energy and (b) high small-scale energy.

Table 3 Results of low small-scale energy test.

\bar{U} (m/s)	1	2	3			
σ_u^2 (m/s) ²	0.021	0.0932	0.212			
\S	1116	1075	1126			
<i>Tree component</i>	f_{res} (Hz)	σ_x^2 (mm) ²	f_{res} (Hz)	σ_x^2 (mm) ²	f_{res} (Hz)	σ_x^2 (mm) ²
Trunk	1.9	1.31E–05	1.9	5.92E–05	1.7	6.43E–04
Bough 1	2.5	1.73E–05	3.2	4.49E–05	3.5	1.73E–04
Bough 2	1.2	1.52E–05	3.5	4.56E–05	3.5	1.64E–04
Petiole	3.7	2.81E–01	3.0	3.99E+00	3.7	2.18E+01

for all tree components is observed, but the petiole movement’s amplitude is five orders of magnitude greater than for other parts (trunk and boughs). Then, an increment of the parameter $S_u(f_{res})/v_{air}$ would produce a small change in the movement’s amplitude of such parts but a big increment of the petiole movement’s amplitude.

3.4. Prototype application

Fig. 6 shows the same result as Fig. 5 but only for the petiole. In such figure are indicated the values of the parameter $S_u(f_{res})/V_{air}$ obtained from prototype measurements in two different sites, identified as A₄ and A₅, inside of the same orchard. In

Table 4 Results of high small-scale energy test.

\bar{U} (m/s)	1	2	3			
σ_u^2 (m/s) ²	0.132	0.728	1.46			
\S	6092	7705	7646			
<i>Tree component</i>	f_{res} (Hz)	σ_x^2 (mm) ²	f_{res} (Hz)	σ_x^2 (mm) ²	f_{res} (Hz)	σ_x^2 (mm) ²
Trunk	1.9	1.20E–04	1.5	1.16E–03	1.6	3.06E–03
Bough 1	3.5	4.55E–05	3.3	8.68E–04	3.1	4.94E–03
Bough 2	3.3	6.15E–05	3.1	8.13E–04	3.2	2.04E–03
Petiole	3.7	1.47E+01	3.5	1.17E+02	4.0	2.96E+02

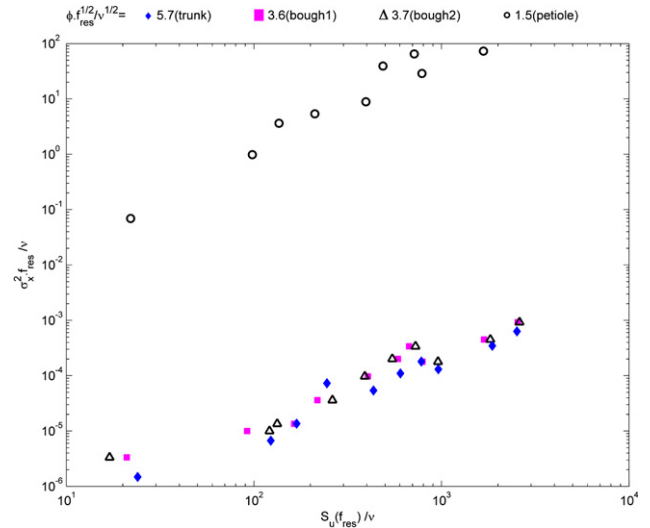


Fig. 5. Dimensionless TKE at petiole’s resonance frequency.

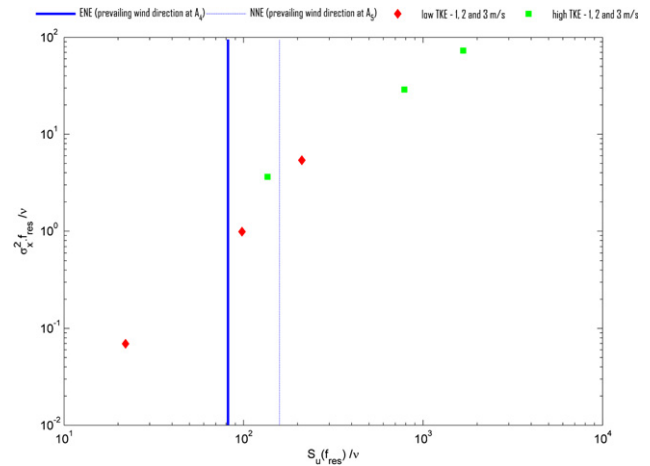


Fig. 6. TKE level at petiole’s resonance frequency, at sites A₄ and A₅.

such sites different small scale turbulence energy levels were determined, as it is indicated in Fig. 6. In the site A₄ the parameter $S_u(f_{res})/V_{air}$ takes a value around 81, while in A₅ such parameter has a value around 156. These values were obtained for the prevailing wind direction in each site inside of the orchard.

From Fig. 6 we could deduce the amplitude of the movement of a petiole in a tree located at the orchard. As an example, in the site A₅ the amplitude of movement of a petiole would be 10 times greater than the movement of the petiole of a tree located at site

A_4 , and as a consequence the contact time, between leaves and fruit, would be greater in site A_4 than in site A_5 .

4. Conclusions

Two typical flow conditions in a citrus orchard were simulated in the wind tunnel, and the responses of a specimen tree were studied. The principal difference between both flow conditions is the energy content at small-scale turbulence.

Comparing the low and high small-scale energy flows, the petiole's movement was found to be the most significant difference in the tree response. Moreover, at the same mean velocity, the petiole's movement presented greater amplitude under a high small-scale energy flow than under a low small-scale energy flow.

Then, the time a leaf would be in contact with an adjacent fruit would be lower for the first case, meaning a lower damage production.

An approach to a theoretical model of a tree response under wind action was proposed to characterize the tree response using information about the wind flow.

The description of the flow inside an orchard could give rise to identify sites where different proportions of damaged fruit would be found, as quoted sites A_4 and A_5 . As site A_4 was found more harmful than A_5 , in terms of discarded fruit (Gravina et al., 2011), we could say that the mechanism that produces damage on fruits is strongly linked with the energy content at small-scales. Moreover, the wind flow that produces more damage would be the one presenting less energy content.

Acknowledgments

This study was mainly funded by the INIA (Spanish for National Institute of Agricultural and Farming Research) and also by the ANII (Spanish for National Agency of Research and Innovation).

Appendix A. Supporting materials

Supplementary data associated with this article can be found in the online version at <http://dx.doi.org/10.1016/j.jweia.2013.01.008>.

References

- Baker, C.J., 1995. The development of a theoretical model for the windthrough of plants. *Journal of Theoretical Biology* 195 (175), 355–375.
- Batchelor, G., 1960. *The Theory of Homogeneous Turbulence*. Cambridge University Press, London 197 pp.
- Brodrick, H.T., 1970. Investigations into blemishes on citrus fruits. *South African Citrus Journal* 441, 7–31.
- Brunet, Y., Fourcaud, T., Achim, A., Belcher, R., Calmet, I., Caltagirone, J.P., Cleugh, H., de Coligny, F., Delavance, M., Druilhet, A., Finnigan, J.J., Foudhil, H., Gamboa-Marrufo, M., Gardiner, B., Guyon, D., Hughes, D., Irvine, M., Lamaud, E., Lohou, F., Lopez, A., Marshall, B.J., Mestayer, P., Morse, A., Paw, K.T., Raupach, M.R., Selier, D., Shaw, R.H., Soulier, D., Wood, C., Yang, B., 2003. The venfor project: wind and forest interactions from the tree scale to the landscape scale. In: *Proceedings of the International Conference: Wind Effects on Trees*, 16–18 September, 2003, University of Karlsruhe, Germany.
- Campbell, M.M., 1967. Windbreaks for citrus trees. *Australian Citrus News* 43 (10), 15.
- Cataldo, J., Pienika, R., Durañona, V., Gravina, A., 2011. Dinámicas del viento en quintas de cítricos y daño en los frutos. *Agrociencia (Uruguay)* 15 (2), 29–39.
- Clough, R.W., Penzien, J., 1993. *Dynamics of Structures*. McGraw Hill Inc., New York 738 pp.
- Dodson, P.G.C., 1966. Damage to citrus fruit by wind. *South African Citrus Journal* 393 (5–7), 11.
- Farell, C., Youssef, S., 1992. Experiments on Turbulence Management Using Screens and Honeycombs. Prepared for NSF, Project Report no. 338, 30 pp.
- Finnigan, J.J., Brunet, Y., 1995. Turbulent airflow in forests on flat and hilly terrain. In: Coutts, M.P., Grace, J. (Eds.), *Wind and Trees*. Cambridge University Press, Cambridge, pp. 3–40.
- Freeman, B., 1976. Artificial windbreaks and the reduction of windscar of citrus. *Proceedings of the Florida State Horticultural Society* 89, 52–54.
- Gardiner, B.A., 1995. The interactions of wind and tree movement in forest canopies. In: Coutts, M.P., Grace, J. (Eds.), *Wind and Trees*. Cambridge University Press, Cambridge, pp. 41–59.
- Gravina, A., 1998. Producción de cítricos para exportación en Uruguay. In: *ANAIS V Seminario Internacional de Citros-Tratos culturales*. Bebedouro, San Pablo, Brasil, pp. 273–288.
- Gravina, A., Espino, M., da Cunha Barros, M., 2005. Evaluación del viento, cortinas de abrigo, sus características y efectos sobre la calidad de los frutos cítricos. II. Análisis del efecto del viento en la calidad externa de los frutos cítricos. In: *2° Simposio de Investigación y Desarrollo Tecnológico en Citrus*. vol. 27. Montevideo, Uruguay. CD, 4p.
- Gravina, A., Cataldo, J., Gambetta, G., Pardo, E., Fornero, C., Galiger, S., Pienika, R., 2011. Relation of peel damage in citrus fruit to wind climate in orchard and its control. *Scientia Horticulturae* 129 (2011), 46–51.
- Green, G.C., 1968. Windbreaks for citrus orchards. *Farming in South Africa* 44 (6), 9–15.
- Groth, J., Johansson, A., 1988. Turbulence reduction by screens. *Journal of Fluid Mechanics* 197, 139–155.
- Holmes, J., 2001. *Wind Loading of Structures*. Spon Press, London.
- James, K.R., Kane, B., 2008. Precision digital instruments to measure dynamic wind loads on trees during storms. *Agricultural and Forest Meteorology* 148, 1055–1061.
- Martínez, D., 1995. Causas de descarte zafra 1995. *Citrus* 27, 18–19. (C.H.N.P.C., MGAP, Montevideo, Uruguay).
- Melbourne, W.H., 1979. Turbulence effects on maximum surface pressures—a mechanism and possibility of reduction. In: Cermak, J.E. (Ed.), *Proceedings of the 5th International Conference on Wind Engineering*. Fort Collins, USA, July 1979, pp. 541–551.
- Moore, J.R., 2002. *Mechanical Behavior of Coniferous Trees Subjected to Wind Loading*. Ph.D. Thesis. Oregon State University, Corvallis, Oregon, USA.
- Moore, J.R., Gardiner, B., Blackburn, G., Brickman, A., Maguire, D., 2005. An inexpensive instrument to measure the dynamic response of standing trees to wind loading. *Agricultural and Forest Meteorology* 132 (2005), 78–83.
- Newland, D., 1984. *An Introduction to Random Vibrations and Spectral Analysis*. Longman Inc., New York 285 pp.
- Owen-Turner, J., Hardy, S., 2006. *Windbreaks for Citrus*. Citrus Fact sheet, Compiled by CITT groups Australia. <<http://www.mvcitrus.org.au>>.
- Popov, E., 1998. *Engineering Mechanics of Solids*, 2nd ed. Prentice Hall, New Jersey 864 pp.
- Richardson, G., 1989. A permeable windbreak: its effect on the structure of the natural wind. *Journal of Wind Engineering and Industrial Aerodynamics* 32, 101–110.
- Richardson, G., Richards, P., 1995. Full-scale measurements of the effect of a porous windbreak on wind spectra. *Journal of Wind Engineering and Industrial Aerodynamics* 54/55, 611–619.
- Ruck, B., Adams, E., 1991. Fluid mechanical aspects of the pollutant transport to coniferous trees. *Boundary-Layer Meteorology*, 163–195 {bf 56}.
- Scarabino, A., 2005. *Características de la Turbulencia Atmosférica en un Bosque de Coníferas*. Ph.D. Thesis. Universidad Nacional de La Plata, Buenos Aires, Argentina.
- Shaw, R.H., 2006. Observation and simulation of flow in vegetation canopies. In: Gayev, Ye.A., Hunt, J.C.R. (Eds.), *Flow and Transport Processes with Complex Obstructions: Applications to Cities, Vegetative Canopies, and Industry*. NATO Science Series, 236. Dordrecht, Netherlands, pp. 179–198.